

Flame Spread along a Thin Combustible Solid with Randomly Distributed Square Pores of Two Different Sizes

Syuhei Abe¹, Akihiko Ito¹ & Hiroyuki Torikai¹

¹ Graduate School of Science and Technology, Hirosaki University, Japan

Correspondence: Akihiko Ito, Graduate School of Science and Technology, Hirosaki University, 3 Bunkyo-cho, Hirosaki 036-8561, Japan. Tel: 81-172-393-679. E-mail: aito@cc.hirosaki-u.ac.jp

Received: July 9, 2012

Accepted: August 6, 2012

Online Published: August 17, 2012

doi:10.5539/mas.v6n9p11

URL: <http://dx.doi.org/10.5539/mas.v6n9p11>

Abstract

The objective of our study is to predict the flame spread route by the quantity of combustible materials and their placement. In this paper, we examine non-uniform flame spread in open air along a thin combustible solid with randomly distributed square pores of two different sizes (8 x 8 and 4 x 4 mm respectively). Experimental results show that the flame-spread probability falls with increasing porosity. Despite uniform porosity, the flame-spread probability differs with the rate of large square pores to small square pores. For a combustible area larger than a noncombustible area, the flame-spread probability reaches the local minimum value with a change in R_g (ratio of 8 mm pores) under the same porosity condition. Conversely, for a combustible area smaller than a noncombustible area, the flame-spread probability reaches a local peak with changing R_g under the same porosity condition. In addition, we calculated the ratio of the unburned area (unburned area / total combustible area) by counting the unburned cells after the flame spread test, which might be useful to predict the fire hazard. We found that the ratio of unburned area grows with increasing porosity.

Keywords: flame spread, solid fuel, flame-spread probability, porosity, percolation theory

1. Introduction

Multiple fires frequently occur in urban areas after a major earthquake. In fact, several fires broke out after the Great Hanshin Earthquake and Great East Japan Earthquake. Urban areas include combustible areas such as wooden structures and plants, as well as noncombustible areas, e.g. concrete buildings, roads, parks, and parking spaces. This means flames spread non-uniformly. In addition, it is difficult to predict the flame spread route because it also depends on the terrain and wind direction. Figure 1 shows photography of some urban area in Japan and a binary image, whereby the urban area is divided into combustible and noncombustible areas. As shown in Figure 1, combustible and noncombustible areas of various sizes are randomly distributed in an urban area. When a fire starts somewhere, one case involves the flame spreading and combustible materials burning out, and the other involves the flame self-extinguishing on the way. The threshold for burning out or self-extinguishing may be determined by the quantity of combustible materials and their placement. Establishing security by predicting the flame spread route is important to save human life in urban fires.

Many studies have been conducted focusing on flame spread along a uniform solid fuel load as a fundamental component of fire research, but few have examined non-uniform flame spread in mixed combustible / noncombustible materials. Recently, a few papers have been published concerning the application of percolation theory to non-uniform flame spread. Percolation theory reveals a probabilistic connection route among particles randomly arranged on a grid, which may or may not be useful in predicting flame spread. A few numerical simulations have also been conducted using a square grid model, however, discussing from an experimental perspective is rare. Therefore, in our previous paper, we conducted experiments concerning flame spread along a thin combustible solid with randomly distributed circle or square pores. We also discussed the relationship between porosity and flame-spread probability based on percolation theory. However, combustible and noncombustible areas vary in respective size in real urban districts, which affects the flame-spread probability and damage by fire, despite the ratios of combustible and noncombustible areas being the same.

In this paper, we studied the flame-spread probability along a thin combustible solid with randomly distributed square pores of various porosity and in two different sizes. In addition, we introduced the ratio of the unburned / combustible area, by counting unburned sample cells after the flame spread test, and discussing the hazard by

fire.

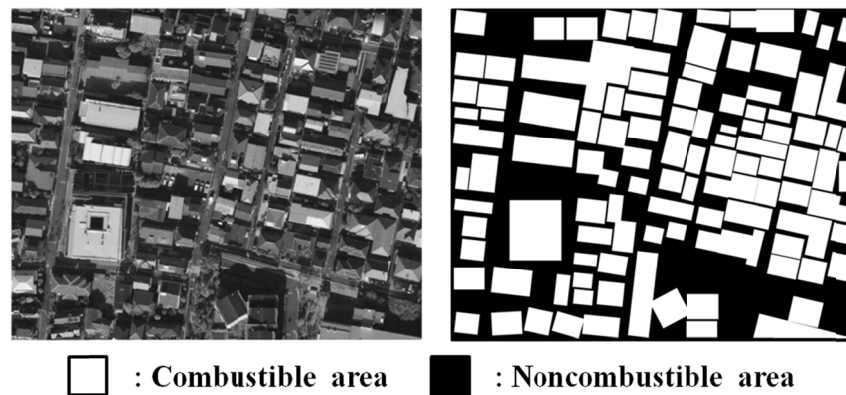


Figure 1. An aerial photo of an urban area and a binary image of the urban area in which combustible and noncombustible areas are divided

2. Experimental Method

2.1 Experimental Apparatus

A schematic of the experimental apparatus and a test sample are shown in Figure 2. In this study, we used a sheet of filter paper as a test sample (ADVANTEC, No. 131). A filter paper was fixed to the aluminum frame, and tensioned to stabilize the flame spread. Thin needles (0.3 mm in diameter) were used to prevent any filter paper fragment surrounded by pores from falling. The end of the test sample was ignited by electrically heated nichrome wire. Experiments were conducted in the atmosphere (oxygen concentration at 21%). A camera (SONY, Handycam, 30 fps) was set up above the test sample to record the top view image of the flame spread. The experiment apparatus was also covered in plastic sheeting to eliminate ambient disturbance to the flame spread.

The test sample was 152 mm long, 56 mm wide and 0.25 mm thick and included pores of different sizes, which opened to establish the non-uniform flame spread. The pore-size was selected with reference to a previous study (Watanabe et al., 2010). In the previous study, the pre-heat length ahead of the flame leading edge along a horizontal filter paper is known to be around 4 mm, and the flame can jump over a 4 mm pore. Flame jumping is related to the pre-heat length, L_h , ahead of the flame leading edge, which means a flame can jump over a pore in $d < L_h$, and not in $d > L_h$ as shown in Figure 3. We introduced the scale ratio $S \equiv d / L_h$ (d : pore-size, L_h : pre-heat length) to classify whether behavior was flame jumping or not, namely whether the flame could jump the noncombustible area for $S < 1$, and not for $S > 1$. In this study, we selected the 4 mm pore-size for $S < 1$, the 8 mm pore-size for $S > 1$, and utilized both pore sizes opened on the test sample. In Figure 2, the 4 mm pores are shown as gray squares, and the 8 mm pores as black squares respectively.

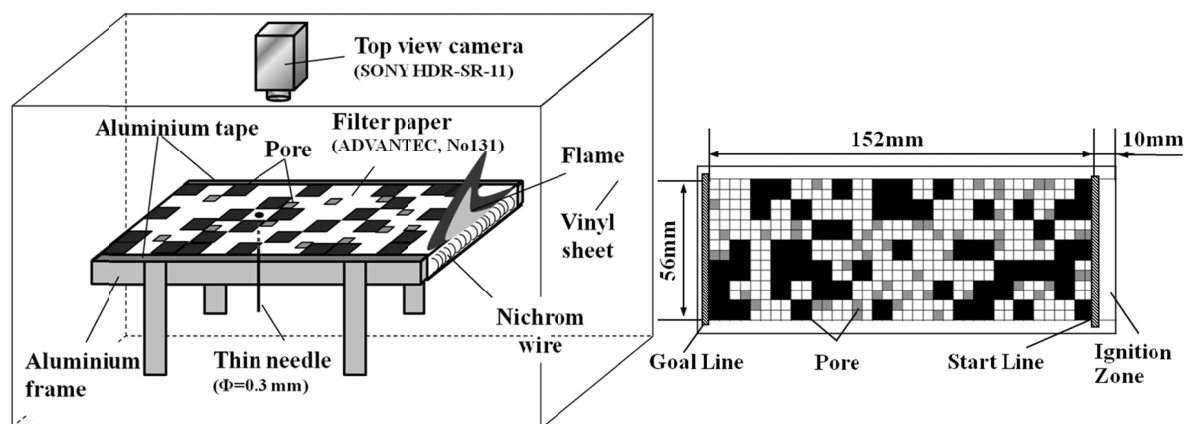


Figure 2. Schematic of the experimental apparatus and the test sample

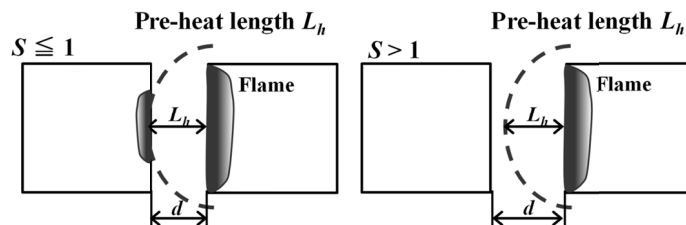


Figure 3. Schematic of flame jumping over a pore

2.2 Porosity and Ratio of the Two Pores of Different Sizes

Based on the percolation theory, the threshold of the flame spread lay at porosity of around 60%, hence we selected five different porosity levels of 40, 45, 50, 55 and 60%. Porosity is defined as Eq. (1), in which the total pore area is obtained by adding a total 4 mm pore area and total 8 mm pore area:

$$\text{Porosity}(P) = \frac{\text{Total pore area}}{\text{Test sample area (length} \times \text{width)}} \times 100\% \quad (1)$$

As shown in Figure 4, some pores interconnect to form what we call a “slit”. Some combustible cells interconnect in a group to form what we call a “combustible cluster”. Some combustible cells or clusters are surrounded by pores, which we refer to as “solitary islands”.

The ratio of pores of two different sizes is given by the ratio of 8mm pore area (larger pore area), R_8 , which is a proportion of the total 8 mm pore area to the total noncombustible area. The ratio of the 8 mm pore area is defined as Eq. (2), in which the total 8 mm pore area is obtained by multiplying the 8 mm pore area by the number of 8 mm pores:

$$\text{Ratio of 8 mm pores area}(R_8) = \frac{\text{Total 8 mm pores area}}{\text{Total noncombustible area}} \times 100\% \quad (2)$$

In this study, we selected seven different R_8 of 100, 92, 88, 80, 67, 57, and 0%. The 100% of R_8 means that all pores are 8 mm square pores, and the 0% of R_8 means that all pores are 4 mm square pores. An example of the test sample with changing R_8 and the same porosity is shown in Figure 5.

2.3 Experimental Condition

We examined 20 types of pore distribution pattern under one experimental condition (i.e., the number of flame spread test is 20 under one experimental condition). The flame-spread probability is defined as Eq. (3), in which the numerator is the number of flame spread from the start line to the goal line.

$$\text{Flame spread probability}(F) = \frac{\text{Number of flame spread success}(N)}{\text{Number of flame spread test}} \times 100\% \quad (3)$$

We obtained the flame-spread probability for five different porosities (40-60%), with seven different ratios of 8 mm pore area (0-100%).

In addition, to discuss the damage by fire, we introduce the ratio of the unburned area to the total combustible area, R_u , which is defined as Eq. (4).

$$\text{Ratio of unburned area}(R_u) = \frac{\text{Unburned area}}{\text{Total combustible area}} \times 100\% \quad (4)$$

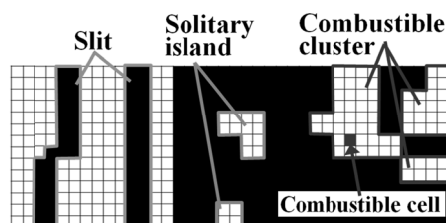


Figure 4. Schematic of a slit, combustible cluster and solitary island

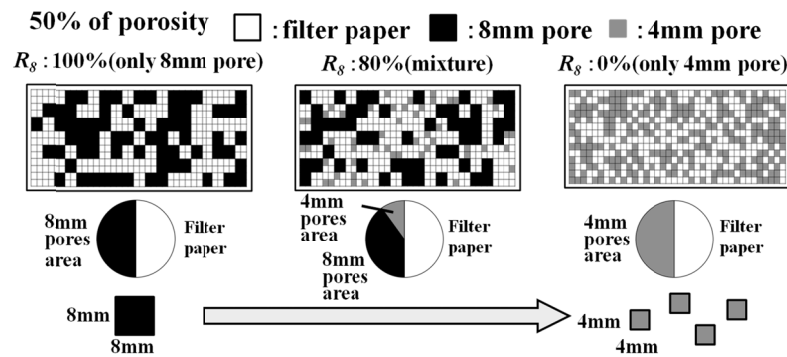


Figure 5. Example of the test sample with changing R_g at the same porosity

3. Results and Discussion

3.1 Flame Spread Trajectory

Figure 6 shows the flame spread trajectory at porosity of 40, 50 and 60% with constant R_g of 67%, respectively. The image processing techniques of flame spread trajectory is normal speed photography (30frames / second). In this figure, the black line is the flame spread trajectory, which is depicted at intervals of two seconds after the flame passed the start line. For 40% porosity, combustible clusters are distributed overall and interconnected, meaning the flame always spreads across the intervening space of combustible materials, as shown in Figure 6a. In the case of 50% porosity, however, the flame sometimes fails to spread across the intervening space of combustible materials, and self-extinguishes on the way as shown in Figure 6b. In the case of 60% porosity, the flame quickly self-extinguishes as shown in Figure 6c. Whether a flame spreads along a test sample or not depends on the presence of some slits on a test sample. These slits are made by connecting each of the pores, which blocks the flame spread and the number of slits grows with increasing porosity. These relationships between pore distribution and flame spread are described in the following section.

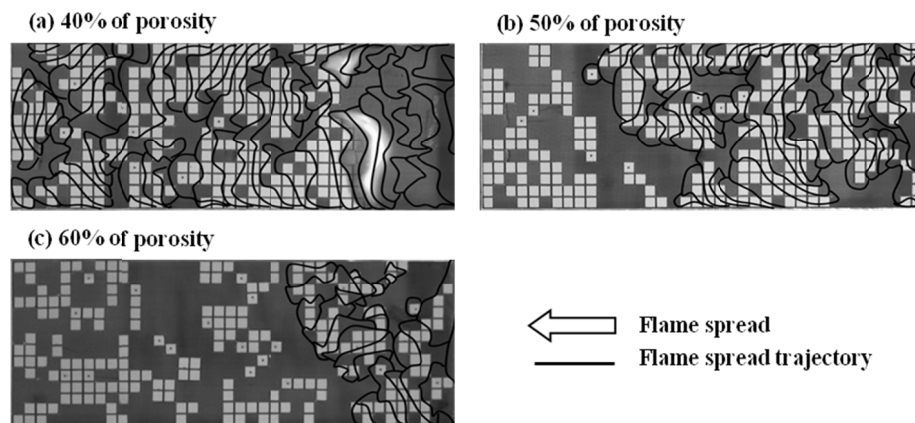


Figure 6. Flame spread trajectory (normal speed photography), (a) at 40% porosity, (b) at 50% porosity, and (c) at 60% porosity with constant R_g of 67%, respectively

3.2 Flame-spread Probability

Figure 7 plots the flame-spread probability as a function of the ratio of the 8 mm pore area to the total noncombustible area for five different porosities. The flame-spread probability changes with changing R_g , despite uniform porosity. The tendency of flame-spread probability to R_g can be roughly divided into the following three regions with porosity. Where the total combustible area exceeds the total noncombustible area (cases of 40 and 45% porosity), the flame-spread probability is convex and downward in shape, with a local minimum value of around 80% of R_g . Where the total combustible area is nearly the same as the total noncombustible area (cases of 50 and 55% porosity), the flame-spread probability is convex, and has a local maximum value at around 67% of R_g . Where the total combustible area is smaller than the total noncombustible area (case of 60% porosity), the flame-spread probability is nearly 0 for all R_g . These differences with R_g did not

emerge in the previous study, because we conducted flame spread experiments with pores of only 4 or 8 mm respectively. In fact, changing the flame-spread probability is not only dependent on porosity but also the ratio of large size porosity ($S > 1$) and small size porosity ($S \leq 1$).

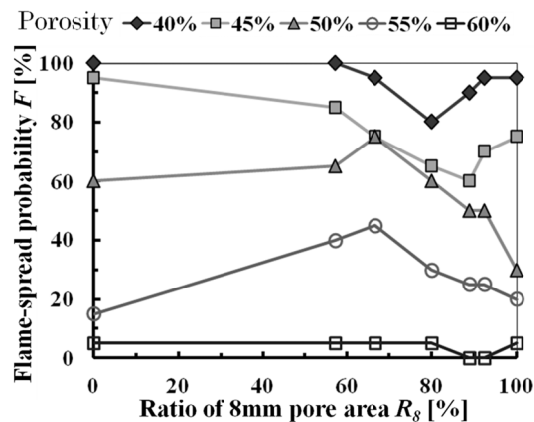


Figure 7. Relationship between the flame-spread probability, F , and the ratio of the 8 mm pore area to the total noncombustible area, R_8

3.3 Relationship between Flame-spread Probability and the Number of Slits

Since the number of slits strongly influences the flame-spread probability, we counted the number of slits made on the test sample under each experimental condition. Figure 8 plots the average number of slits, N_s , as a function of R_8 for five different porosities. In this figure, the N_s is significant as a large porosity value. In detail, the number of slits changes with changing R_8 at the same porosity. The tendency of N_s with porosity is characterized into the following three categories:

Firstly, for porosity of 40 and 45%, it is easy for combustible cells to interconnect because there are more combustible cells than pores. As shown in Figure 9a, combustible cells interconnect and the flame can spread along combustible materials at R_8 of 100 and 0%. However, at 80% of R_8 , some 8 mm pores are substituted for 4 mm pores. These 4 mm pores are distributed within the connection space of combustible cells and a slit is formed. The flame cannot jump over this slit and self-extinguishes on the way. As a result, the flame-spread probability declines.

Secondly, in the case of porosity at 50 and 55%, some slits form easily because the number of pores exceeds that of combustible cells. As shown in Figure 9b, the flame may not spread across the test region because the test sample has some slits at 100%, 0% of R_8 . Conversely, at 67% of R_8 , some combustible clusters and combustible cells are distributed on the test sample. These small combustible cells were distributed on the test sample overall, and combustible cells interconnected. As a result, the flame spread route was formed and the flame-spread probability increases.

Finally, in the case of 60% porosity, almost two slits are formed at all R_8 . Additionally, even though small combustible cells are distributed overall, the test sample may lack a flame spread route because the number of pores is far larger than that of combustible cells. Eventually the flame self-extinguishes on the way under all experimental conditions, and the flame-spread probability reaches nearly 0%.

Similar tendency was shown in other literature (Sekine, 1976). Sekine conducted fire spread experiment by using wood crib (profile: 3.6 x 3.6 cm and length: 1 m, quintuple stack) and found the threshold of flame spread is 60% porosity. In addition, connecting threshold of percolation theory is approximately 60%. Through these results, we suggest that we can predict the fire spreads or self-extinguishes from porosity by using percolation theory.

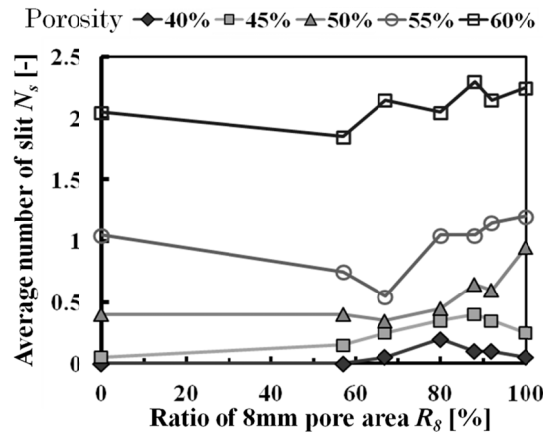


Figure 8. The average number of slits as a function of R_8 for five different porosities

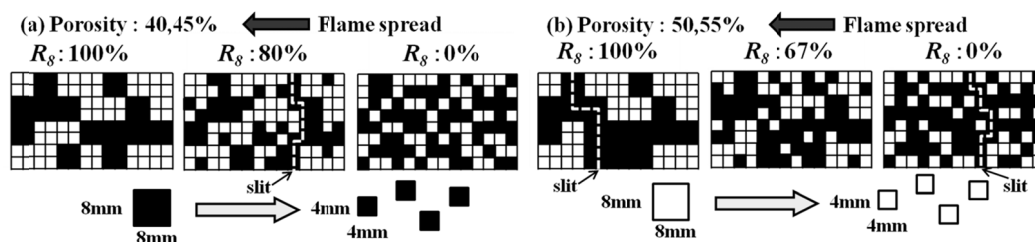


Figure 9. Different circumstances based on the presence or absence of a slit, (a) slit is made by small pores distributed, and (b) a flame spread route is formed by small combustible cells distributed

3.4 Ratio of Unburned Area

Predicting the extent of combustible area surviving after the flame spread is important when estimating fire hazard, which is why we introduce the ratio of unburned area to total combustible area, R_u . Figure 10 plots the R_u as a function of R_8 . In this figure, the broken line indicates the average value of R_u at each porosity. Although R_u increases overall with increasing porosity, it differs with the value of R_8 . In particular, the difference of R_u is striking when R_8 is large with porosity of 45 - 55%. This difference is considered due to the existence or non-existence of slits as shown in Figure 11. When flame self-extinguishes on the way due to slits, many combustible cells are unburned as shown in Figure 11a. Even though the flame spreads from the start line to the goal line, some isolated combustible clusters survive as shown in Figure 11b. Accordingly, the R_u is determined by the two types of survival method of combustible area.

With 40% of porosity, it is difficult for the test sample to have a slit because the number of combustible cells exceeds that of pores, meaning a flame can easily spread to goal line. In addition, there are almost no solitary islands. The amount of combustible area surviving decreases and the R_u declines. With porosity of 45 - 55%, the test sample can have a slit. When a slit is formed, the amount of survival combustible area increases more than when no slit is present, meaning the R_u differs at the same porosity. With 60% porosity, almost two slits are formed on the test sample and the probability that a slit is formed near the start line grows with an increasing number of slits. When a slit forms near the start line, the flame may quickly self-extinguish and many combustible areas survive.

As shown in Figure 10, at R_8 of 92%, we found that the R_u exceeds the average value of R_u for all porosities, whereas at R_8 of 57%, R_u is lower than the average value of R_u for all porosities. Figure 12 shows a schematic of the test sample with R_8 at 92 and 57%. With R_8 of 92%, the number of 8 mm pores, N_8 , is three times more than the number of 4 mm pores, N_4 ($N_8 : N_4 = 3 : 1$). Under this condition, large combustible clusters exist on the test sample. When a slit is formed, some combustible clusters distributed after the slit may survive. Additionally, the test sample also contains some solitary islands, meaning the value of R_u exceeds the average value. Conversely, with R_8 of 57%, N_4 is three times larger than N_8 ($N_8 : N_4 = 1 : 3$). Under this condition, the combustible cells are

distributed overall on the test sample. The flame spread route is easily formed with connecting combustible cells, and flames can spread across the intervening space of combustible materials. As a result, the value of R_u is lower than the average value for all porosities. From a fire-safety perspective, an urban area may have suffered most damage by fire, where the number of small spaces ($S \leq 1$) is three times larger than that of large spaces ($S > 1$) when the sum total of spaces is the same.

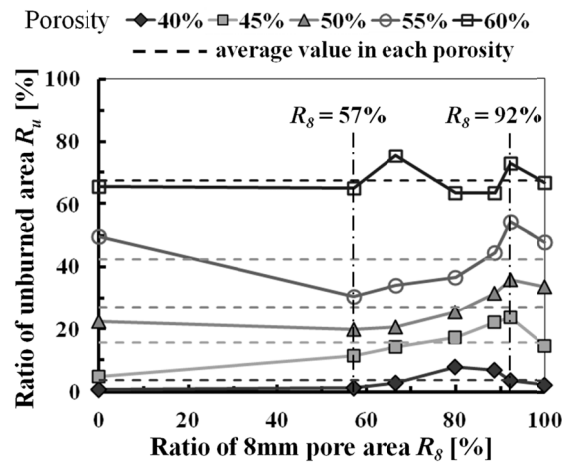


Figure 10. Relationship between the ratio of unburned area to total combustible area, R_u , and the ratio of 8 mm pore area to total noncombustible area, R_g

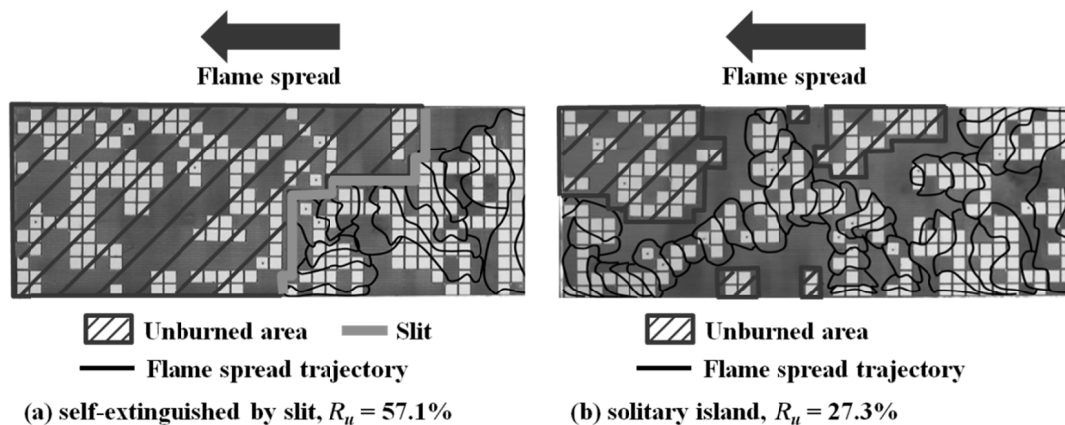


Figure 11. Different situations of the unburned combustible area; (a) flame not spread by slits and combustible materials unburned, and (b) flame spread but the solitary isolated are unburned

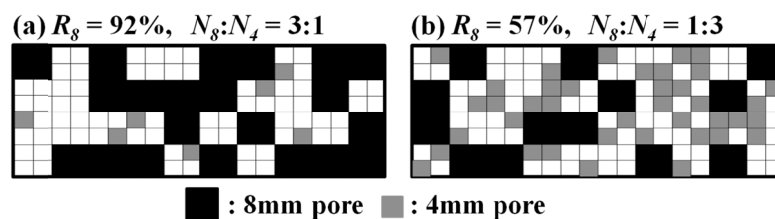


Figure 12. Schematic of the test sample at R_g of 92 and 57%. The proportion of the N_g and N_4 differs with R_g , (a) $N_g : N_4 = 3 : 1$, and (b) $N_g : N_4 = 1 : 3$

4. Conclusion

In this study, we conducted flame spread experiments using a sheet of filter paper with pores of two different

sizes randomly distributed. The following conclusions can be summarized here:

- 1) The flame-spread probability decreases with increasing porosity. However, with changing R_8 at the same porosity, the flame-spread probability reaches the local minimum and maximum values at around 40 and 50% porosity respectively. At 60% porosity, some slits are formed and the flame-spread probability becomes nearly 0%. This tendency is similar to the threshold of percolation theory, meaning flame spread can be discussed in terms of percolation theory.
- 2) The average number of slits, N_s , grows with increasing porosity ranging from 40 to 60%. However, N_s differs with different R_8 at the same porosity. This difference is considered attributable to the presence or absence of a slit. For porosities of 40 and 45%, a slit is formed by distribution of small pores at R_8 of around 80%. For porosities of 50 and 55%, the flame spread route is formed by the distribution of combustible cells at R_8 of around 67%. For 60% porosity, almost two slits are formed for all R_8 . In fact, the flame-spread probability falls with increasing N_s .
- 3) The ratio of unburned area to total combustible area grows with increasing porosity. This tendency is observed in all R_8 . However, under the same porosity condition, the R_u differs with R_8 . The value of R_u at 92% of R_8 peaks, and the value of R_u at 57% of R_8 has a minimum value for all porosities. We suggest that the fire hazard in urban areas is most dangerous where the number of noncombustible small spaces is three times larger than that of large spaces.
- 4) The ratio of unburned area large increases around 60% porosity for all of R_8 . From a fire-safety perspective, it is advisable that the ratio of noncombustible area raise more than 60% relative to an urban area. Furthermore we should place the combustible materials in an urban area with spacing which fire cannot jump over.

Acknowledgments

We would like to thank Y. Watanabe and S. Kudo for their help in experiments and in preparing the manuscript.

Nomenclature

d	pore-size (diameter of the side of the square pore)
F	flame-spread probability
F_j	flame jumping probability
L_h	pre-heat length ahead of the flame leading edge
N	number of flame spread
N_4	number of 4 mm pores
N_8	number of 8 mm pores
N_j	number of flames jumping
N_s	average number of slits
P	porosity
R_8	ratio of 8 mm pore area
R_u	ratio of unburned area
S	scale ratio ($\equiv d / L_h$)

References

- De Ris, J. (1969). The spread of a laminar diffusion flame, twelfth Symposium (Int.) on Combustion. The Combustion Institute, pp. 241-252.
- Di Blasi, C. (1994). Processed of Flames Spreading Over the Surface of Charring Fuels: Effects of the Solid Thickness. *Combust Flame*, 97, 225-239. [http://dx.doi.org/10.1016/0010-2180\(94\)90006-X](http://dx.doi.org/10.1016/0010-2180(94)90006-X)
- Fernandez-Pello, A. C., & Williams, F. A. (1977). A Theory of Laminar Flame Spread Over Flat Surfaces of Solid Combustibles. *Combustion and Flame*, 28, 251-277. [http://dx.doi.org/10.1016/0010-2180\(77\)90032-3](http://dx.doi.org/10.1016/0010-2180(77)90032-3)
- Fernandez-Pello, A. C., & Hirano, T. (1983). Controlling Mechanisms of Flame Spread. *Combust. Sci. Technol.*, 32, 1-31. <http://dx.doi.org/10.1080/00102208308923650>
- Ito, A., & Kashiwagi, T. (1988). Characterization of flame spread over PMMA using holographic interferometry sample orientation effects. *Combustion and Flame*, 71(2), 189-204. [http://dx.doi.org/10.1016/0010-2180\(88\)90007-7](http://dx.doi.org/10.1016/0010-2180(88)90007-7)

- Kokubo, S., Yamamoto, K., Yamashita, H., & Nishinari, K. (2007). Simulation of evacuation dynamics in fire, Proceeding of the North-fifth Symposium (Japanese) on Combustion, pp. 488-489.
- Kugai, T., Kato, T., & Koide, O. (2001). The basic study on the evaluation of disaster mitigation performance of the local area road network based on Percolation theory (in Japanese). *Journal of Architecture, Planning and Environmental Engineering*, 549, 231-237.
- Oyagi, H., Shigeno, H., Mikami, M., & Kojima, N. (2009). Flame-spread Probability and Local Interactive Effects in Randomly Arranged Fuel-droplet Arrays in Microgravity. *Combustion and Flame*, 156(4), 763-770. <http://dx.doi.org/10.1016/j.combustflame.2008.12.013>
- Sato, K., Hirano, T., & Miki, K. (1984). Flame spread over paper in an air stream with a velocity change. *J. Heat Transfer, ASME*, 106, 7070-712. <http://dx.doi.org/10.1115/1.3246742>
- Sekine, T., & Unno, K. (1976). Experimental Study on Spatial Structure of Airflow around Buildings in Urban Area: Part I. Investigations on the characteristics of airflow around regularly arranged city models (in Japanese). *Architectural Institute of Japan*, 245, 113-122.
- Stauffer, D. (1985). Introduction to Percolation Theory. London: *Taylor and Francis*. <http://dx.doi.org/10.4324/9780203211595>
- Stauffer, D., & Aharony, A. (1992). Introduction to Percolation Theory (second ed.). *Taylor & Francis*, London, Washington DC.
- Umemura, A. (2011). Application of Percolation Theory to Combustion Problems. *Journal of the Combustion Society of Japan*, 53(165), 145-152.
- Watanabe, Y., Ito, A., & Torikai, H. (2009). Effect of Porosity on Flame Spread along a Thin Combustible Solid Randomly Distributed Pores. Sixth International Symposium on Scale Modeling, Proceedings.
- Watanabe, Y., Ito, A., & Torikai, H. (2010). Flame spread along a thin randomly distributed combustible and noncombustible areas. 33th International Symposium on Combustion.